Available online at www.sciencedirect.com
ScienceDirect
Journal of Solid State Chemistry 179 (2006) 3591–3598
JOURNAL OF SOLID STATE CHEMISTRY
www.elsevier.com/locate/jssc

Hydrothermal synthesis and structure determination of the new vanadium molybdenum mixed oxide $V_{1.1}Mo_{0.9}O_5$ from synchrotron X-ray powder diffraction data

F. Duc[a,*], S. Gonthier[a], M. Brunelli[b], J.C. Trombe[a]

[a]CEMES/CNRS, 29 rue J. Marvig, B.P. 94347, 31055 Toulouse Cedex 4, France
[b]European Synchrotron Radiation Facility, B.P. 220, F-38043 Grenoble, France

Received 27 April 2006; received in revised form 13 July 2006; accepted 16 July 2006
Available online 20 July 2006

Abstract

A new vanadium molybdenum mixed oxide $V_{1.1}Mo_{0.9}O_5$ [$V(V)_{0.2}V(IV)_{0.9}Mo(VI)_{0.9}O_5$] has been synthesized, as a pure phase, via hydrothermal methods in the presence of molybdic acid and vanadyl sulfate. Its crystal structure has been solved ab initio from high-resolution powder diffraction data collected at the ESRF beamline ID31. This compound crystallizes in the monoclinic symmetry, space group $C2/m$, with cell dimensions $a = 12.1230(2)$ Å, $b = 3.7168(1)$ Å, $c = 4.0336(1)$ Å, $\beta = 90.625(3)^\circ$ and $Z = 2$ per formula. The structure consists of double strings of VO_5 square pyramids sharing edges and corners along [100] and [010], and more weakly bound along [001]. In this latter direction, the bond (V,Mo)–O = 2.377 Å, while remaining long, leads for the first time to the interpenetration of the apical oxygens of the $[(V,Mo)_2O_5]_n$ layers, resulting in a three-dimensional (3D) structure closely related to R-Nb_2O_5. This structure will be compared to the pure layer structure of V_2O_5 where this bond reaches 2.793 Å.
© 2006 Elsevier Inc. All rights reserved.

Keywords: Vanadium oxides; Mixed valence oxides; Hydrothermal synthesis; Powder diffraction

1. Introduction

For many years, the substitution or insertion of various M cations (from alkalies or alkaline-earths to metals) in the V_2O_5 layered structure has been investigated by means of solid-state reaction. In addition to the discovery of the wide vanadium oxide bronze family $M_xV_{2-x}O_5$, another field has been particularly highlighted: the substitution of the Mo(VI) + V(IV) couple for 2 V(V) in the $M_xV_{2-x}O_5$ and V_2O_5 structures, leading to the first mixed vanadium bronzes $M_xV_{2-y}T_yO_5$ (with $M = Li$, Na and $T = Mo$, W)) [1–5] and to the $V_{2-x}Mo_xO_5$ phases ($0 \leqslant x \leqslant 1$) [2–7]. Within this range, the cell parameters of the last phases exhibit several discontinuities associated with symmetry changes. Recently, these phases have been re-investigated and the homogeneity ranges, the crystal structure and the physical properties of each solid solution have been determined more accurately [8].

For a long time, most of this research has been carried out by traditional high temperature solid-state chemistry [9]. Hydrothermal techniques, extensively used for the synthesis of zeolite materials and open-framework structures, have only since the last 10 years been explored for the synthesis of new transition metal oxides. The synthesis of new related compounds of vanadium oxides [10,11] has in particular attracted much interest due to their numerous chemical (catalysis) [12,13] and physical (magnetism, conductivity, optic) properties. The results showed the relevance of this soft chemistry approach since new materials can be obtained that often cannot use solid-state reactions at high temperature. Recently, we tried this approach to grow single crystals of the tetragonal $VMoO_5$ phase [14]. This compound, which is often written as $VOMoO_4$, is currently receiving significant attention by the scientific community because of its magnetic properties. It is considered one of the first prototypes of the frustrated

*Corresponding author. Fax: +33 5 62 25 79 99.
E-mail address: fduc@cemes.fr (F. Duc).

0022-4596/$ - see front matter © 2006 Elsevier Inc. All rights reserved.
doi:10.1016/j.jssc.2006.07.018

two-dimensional (2D) $S = 1/2$ antiferromagnets on a square lattice [15–18]. Unfortunately, the growth of single crystals with useful size for physical measurements is difficult to achieve. Moreover, most of the crystals prepared by chemical transport reaction at 575–600 °C are twinned, hence our aspiration of improving the quality of $VMoO_5$ single crystals by means of hydrothermal synthesis. In that purpose we failed but this work made it possible to isolate a new monoclinic $V_{1.1}Mo_{0.9}O_5$ phase.

In this paper, the synthesis and the structure determination of this new phase, based on high-resolution synchrotron radiation powder diffraction data, are reported. Its structure will be compared with those of the orthorhombic V_2O_5 [19] and monoclinic $V_{1.4}Mo_{0.6}O_5$ [6] phases.

2. Experimental section

2.1. Synthesis

The title compound was prepared by hydrothermal synthesis under autogeneous pressure. An aqueous suspension (10 mL) of molybdic acid (0.94 mmol) and vanadyl sulfate (1 mmol), to which a small quantity of arsenic pentoxide (in a molar ratio $V/As = 8$) was added, was heated in a Teflon-lined stainless steel autoclave. A typical synthesis requires heating at 200 °C for 30 days followed by a slow cooling to room temperature. The powder was filtered, washed with distilled water and air-dried at room temperature. Monophasic crystalline material was confirmed by X-ray powder diffraction. The chemical analysis led to the following values: % calculated on the basis of a stoichiometric formula $MoVO_5$: Mo 42.28; V 22.45; % found Mo 40.5; V 21.0, giving an atomic ratio Mo/V approximately 1/1. Taking the synthesis method and particularly the drying process into account, it seems likely that the samples could contain some adsorbed water, which would explain the deficit of metals. Energy dispersive X-ray (EDX) analysis performed on several crystallites in a transmission electron microscope and inductively coupled plasma mass spectrometry (ICPMS) measurements confirmed firstly the absence of arsenic in the compound and secondly that the atomic ratio of Mo/V was around $1/1 \pm 0.1$. The As_2O_5 which does not enter the solid improves greatly the crystallinity of the sample and therefore could be considered as a mineralizer.

Before obtaining this particular result, some experiments were performed in order to determine the relevant factors to get this new phase, still with the hydrothermal technique. The first ones were carried out using an aqueous suspension of V_2O_5 plus MoO_3 ($V/Mo = 1$) in the presence of a reduction reagent like hydrazine dihydrochloride to afford the reduction of the V(V) to the V(IV). The pH value of the final solution must range between 1 and 2; the temperature and time treatment must be as high as possible, from 150 to 220 °C for several weeks, respectively. However, the X-ray powder patterns of the solids, arising from these first experiments, were most of the time characteristic of a mixture of several phases including the required phase. Instead of the molybdenum and vanadium oxides, the use of more soluble precursors, such as molybdic acid and vanadyl sulfate, was tried through the range of an atomic ratio V/Mo from 1 to 2, the excess of vanadyl sulfate being carried away in the final solution and the washed water. This way made it possible to get the same phase as the one quoted above. However, depending on the synthesis conditions, the powders obtained were more or less well crystallized. In order to improve the latter factor, the fluoride route, a well-known mineralizer, and the effect of the addition of some reagents like NH_4Cl and As_2O_5 were checked (Table 1). The best results were observed with the latter reagent; however, no single crystals were obtained.

2.2. High-resolution synchrotron powder diffraction data

As no suitable single crystals were obtained, a structure determination from X-ray powder diffraction (XRPD) data was performed. XRPD patterns were collected at the high-resolution powder X-ray diffractometer at the beamline ID31 at ESRF, Grenoble, France [20]. Dark gray powdered sample was gently ground in an agate pestle-mortar and then loaded in a 0.9 mm diameter borosilicate glass capillary; the capillary was mounted on the axis of the diffractometer and spun at 50 Hz during measurements in order to improve powder randomization. A wavelength of $\lambda = 0.20650(1)$ Å was selected with a double-crystal Si(111) monochromator. Data were collected overnight in a continuous scan mode up to 30° (2θ). Diffracted intensities were detected through one Si(111) analyser crystal.

The extraction of peak positions for indexing was performed with the software package WINPLOTR [21]. Pattern indexing was carried out by means of the program DICVOL04 [22]. The program EXPO [23] was used for structure solution and FULLPROF [24], available in the software package WINPLOTR [21], for structure refinement by the Rietveld method. The program DIAMOND (version 3.1a) from Crystal Impact [25] was used for structure drawings.

3. Ab initio structure determination

3.1. Pattern indexing

The phase identification, from the Powder Diffraction File database, revealed that the powder diffraction pattern was similar to that of two compounds.

The first compound proposed is the $V_{0.95}Mo_{0.97}O_5$ phase [26] (PDF-2 No. 77-0649) which has been described in the triclinic space group $P1$ ($a = 6.3340(5)$ Å, $b = 4.0463(5)$ Å, $c = 3.7255(5)$ Å, $\alpha = 90.0(1)°$, $\beta = 107.3(1)°$ and $\gamma = 90.5(1)°$). Although the structure of this material was solved in a triclinic symmetry, the authors suggested that the symmetry could be monoclinic. Actually, their powder pattern showed overlap for most of the peaks which

Table 1
Synthesis conditions of some selected experiments which resulted in a pure phase

Ref. No.	T (°C)	Duration (days)	Nature of the reagents	pH	Color of the final solution	Cell parameters
2672	220	30	$1VOSO_4 + 1H_2MoO_4 + 2NH_4Cl + 5$ ml H_2O	1.3	Nearly colorless	$a = 12.111(4)$ Å $b = 3.717(1)$ Å $c = 4.0309(1)$ Å $\beta = 90.65(2)^\circ$ $V = 181.5$ Å^3
2674	220	30	$1VOSO_4 + 1H_2MoO_4 + 2HF + 5$ ml H_2O	2.2	Pale blue	$a = 12.135(2)$ Å $b = 3.724(1)$ Å $c = 4.0329(5)$ Å $\beta = 90.63(2)^\circ$ $V = 182.2$ Å^3
2559	220	40	$1.5VOSO_4 + 1H_2MoO_4 + 10$ ml H_2O	1.2	Blue	$a = 12.099(6)$ Å $b = 3.714(1)$ Å $c = 4.032(1)$ Å $\beta = 90.58(3)^\circ$ $V = 181.2$ Å^3
2350	200	4	$2VOSO_4 + 1H_2MoO_4 + 10$ ml H_2O	1.0	Blue	$a = 12.065(4)$ Å $b = 3.706(1)$ Å $c = 4.042(1)$ Å $\beta = 90.66(3)^\circ$ $V = 180.7$ Å^3
2351	200	16	$2VOSO_4 + 1H_2MoO_4 + 10$ ml H_2O	2.0	Blue	$a = 12.071(5)$ Å $b = 3.708(1)$ Å $c = 4.042(2)$ Å $\beta = 90.66(3)^\circ$ $V = 180.9$ Å^3
2560	220	40	$1VOSO_4 + 0.94H_2MoO_4 + 0.06As_2O_5 + 10$ ml H_2O	1.2	Nearly colorless	*$a = 12.124(1)$* Å *$b = 3.7165(4)$* Å *$c = 4.0323(4)$* Å *$\beta = 90.61(1)^\circ$* *$V = 181.7$* Å^3
2670	220	30	$1VOSO_4 + 1H_2MoO_4 + 0.25As_2O_5 + 5$ ml H_2O	1.7	Pale blue	$a = 12.123(1)$ Å $b = 3.7184(4)$ Å $c = 4.0319(4)$ Å $\beta = 90.62(1)^\circ$ $V = 181.7$ Å^3

The cell parameters determined with DICVOL04 [22] are reported in the last column. The preparation referred to by the number 2560 led to the sample studied in this work.

induced considerable difficulties to determine and refine the unit-cell parameters.

Despite a small shift of all X-ray reflections, the powder pattern of our compound is also close to that given for $V_{1.4}Mo_{0.6}O_5$ (PDF-2 No. 73-1822, $a = 11.809(2)$ Å, $b = 3.652(1)$ Å, $c = 4.174(1)$ Å and $\beta = 90.56(2)^\circ$), in which the crystal structure has been determined by single-crystal diffraction methods in the space group $C2$ [6]. This compound is considered as the molybdenum highest limit at 650 °C of the solid solution $V_{2-x}Mo_xO_5$ ($0.48 \leqslant x \leqslant 0.60$) [3,6,8].

Aware of this latter possibility for the indexation, the angular positions of the first 35 diffraction lines, with an absolute error of 0.02° (2θ), were used for indexing the pattern on the basis of a monoclinic cell. The unit cell dimensions refined from the diffraction lines available are listed in Table 2 together with the high figures of merit M_{20} and F_{35} [27]. From the analysis of the indexed powder data, the systematic absences suggested the space groups $C2$, Cm, $C2/m$, $P2_1/a$.

3.2. Structure determination and refinement procedure

Integrated intensities were extracted with the iterative pattern decomposition algorithm available in EXPO and were subsequently used to solve the structure. The range of

Table 2
Crystallographic data and details of the Rietveld refinement for the monoclinic $V_{1.1}Mo_{0.9}O_5$ phase

Crystal system	Monoclinic
Space group	$C2/m$
a (Å)	12.1230(2)
b (Å)	3.7168(1)
c (Å)	4.0336(1)
β (deg)	90.625(1)
V (Å^3)	181.73(1)
Formula weight (g mol^{-1})	222.57
Z	2
ρ_{calc} (g cm^{-3})	4.067
M_{20}	39
F_{35}	175.8 (0.0012, 169)
Wavelength (Å)	0.2065
2θ range (°)	1.10–30
Step scan increment (°2θ)	0.005
No. of reflections	1823
No. of structural parameters	12
No. of profile parameters	11
No. of global parameters	1
No. of atoms	5
R_F	0.063
R_B	0.048
R_p	0.230
R_{wp}	0.206
R_{exp}	0.187

For the definition of agreement factors from the Rietveld refinement, see Ref. [24].

1.48–18.37° (2θ) offered a reasonable compromise between the number of reflections (400) and the number of statistically independent reflections (44%), according to the degree of diffraction line overlap [28]. The structure factor amplitudes thus obtained were used for the structure determination with the direct methods available in the software. Attempts to solve the structure were made in the four possible space groups. The refinements of the structural models obtained in the space groups Cm and $P2_1/a$ were not conclusive and were then disregarded. In the space group $C2/m$, the structural model supplied by the program EXPO was built up by four atoms and led to a residual R factor of 0.13. At this stage, there were one Mo atom, lying on a mirror plane, and three O atoms, two of them being located on a mirror plane and one at the inversion center (position 2a: 0,0,0). However, the Fourier map calculated from the solution indicated that the number of electrons estimated for the Mo atom was equal to 35 instead of 42. Since no site was proposed for the V, this result was attributed to a mixed occupancy Mo/V of this site. Consequently, taking the results of the analysis into account, it was assumed that the Mo site was occupied by 50% of V and 50% of Mo. This solution was then used as a starting structural model for a Rietveld refinement based on the whole angular range 1.10–30° (2θ). A pseudo-Voigt function convoluted with the axial divergence asymmetry correction proposed by Finger et al. [29] was selected to describe individual line profiles. The background was adjusted with a linear interpolation between refined intensity points. The atomic coordinates and the temperature factors of Mo and V atoms were constrained to be equal. The occupancy factors of the Mo/V sites were first fixed and restrained to a total content of two metal atoms per chemical formula. Since the absorption correction coefficient ($\mu R = 0.32$) was low, no absorption correction was applied. In the final cycles, besides the scale factor, the zero-point and the profile parameters, the unit cell parameters, the variable atomic coordinates, the isotropic temperature parameters and the Mo/V occupancy factors were refined.

The details of the Rietveld refinement are given in Table 2. Fig. 1 shows the final fit between observed and calculated pattern. Final atomic parameters are given in Table 3 and selected distances and angles calculated with the BONDSTR program are reported in Table 4.

The structural model supplied in $C2$ was similar to the one obtained in $C2/m$ with one site with a mixed Mo/V occupancy and three O sites. In spite of reliability factors slightly smaller in $C2$ ($R_F = 0.052$, $R_{Bragg} = 0.045$, $\chi^2 = 1.06$), the refinement in this space group was essentially the same. The better fit obtained in $C2$ was essentially due to more freedom to move the atoms along [010]. Indeed, whereas the oxygen atoms were located on the 2a and 4i positions in $C2/m$ constraining the y coordinates at 0 and 1/2, they were positioned on the 2a and 4c sites in $C2$ leaving the y coordinates free to vary. In this space group, the O atoms O1, O2 and O3 were therefore found, respectively, at $y = 0.0104$, 0.4988 and -0.0124 emphasizing that these atoms are only slightly displaced from their positions fixed by symmetry in $C2/m$. For these reasons, we have chosen $C2/m$ as the final space group.

3.3. Discussion and conclusion

The chemical formula derived from the site occupancies is $V_{1.1}Mo_{0.9}O_5$ in rather good agreement with the one from the chemical analysis. However, this result leads to the following cationic formulation $[V(V)_{0.2}V(IV)_{0.9}Mo(VI)_{0.9}O_5]$ highlighting the presence of V(V) in the compound. This fact could be explained by the oxidation of a small amount of V(IV) during the synthesis process as it has already been observed in other hydrothermal treatments of $VOSO_4$ aqueous solution [10,30].

The structure obtained is very similar to that of $V_{1.4}Mo_{0.6}O_5$ [3,6]. It is built up of $[M_2O_5]_n$ layers (M = Mo, V) sharing edges and corners in the (a, b) plane but now connected by apices in the [001] direction, making a 3D network as in R-Nb_2O_5 [31] by the evolution of the MO_5 square pyramids into MO_6 octahedra. A comparative view of the (a, c) plane of the V_2O_5, $V_{1.4}Mo_{0.6}O_5$, $V_{1.1}Mo_{0.9}O_5$ and R-Nb_2O_5 structures is reported in Fig. 2. It gives an overview of how the stacking of the $[M_2O_5]_n$ layers changes with the Mo composition. According to the previous studies [3,6,8], the progressive replacement of vanadium by molybdenum gives rise to a solid

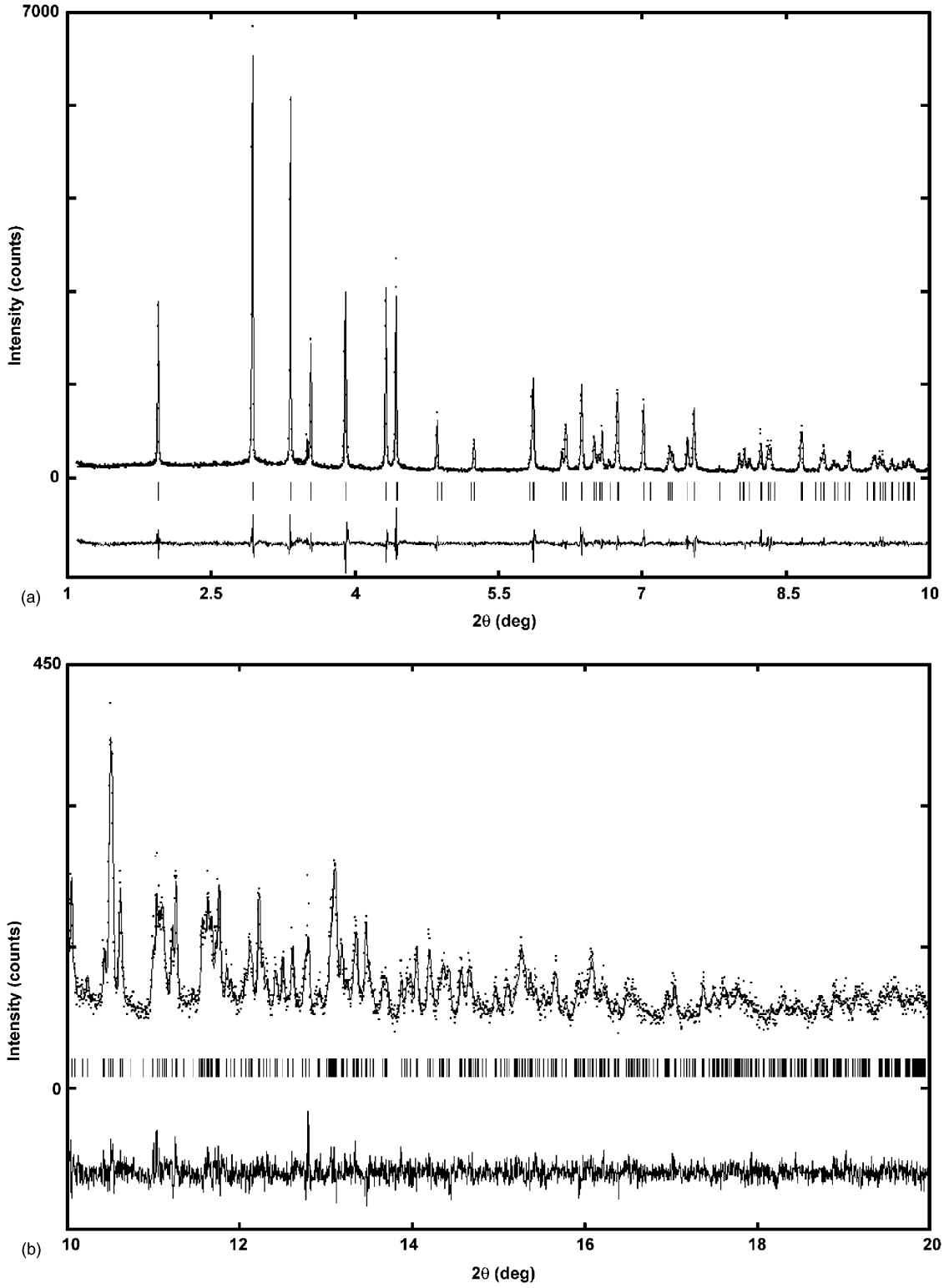

Fig. 1. Final Rietveld plot for the monoclinic $V_{1.1}Mo_{0.9}O_5$ phase in the low (a) and high (b) angular ranges. The experimental data are represented by dots, while the calculated pattern is shown by the solid line. The lower trace corresponds to the difference between observed and calculated pattern. The positions of the Bragg reflections are shown by the vertical lines.

solution, the $V_{2-x}Mo_xO_5$ phases, for which the homogeneity range at 650 °C has been determined to extend up to $x = 0.60$. Moreover, these investigations have shown that the variations of the unit cell dimensions with the substitution of molybdenum for vanadium exhibit two discontinuities associated with symmetry changes. For the compositions $0 \leqslant x \leqslant 0.36$, the phases are isostructural with the orthorhombic V_2O_5, whereas a decrease of symmetry is

detected for the phases with a homogeneity range $0.48 \leqslant x \leqslant 0.60$. Hence, their structure becomes monoclinic and is expected to be similar to the one of the $V_{1.4}Mo_{0.6}O_5$ compound. In the range $0.36 \leqslant x \leqslant 0.48$, a mixture of both kinds of border phases is observed. The evolution of the cell parameters of the $V_{2-x}Mo_xO_5$ phases with the composition ($0 \leqslant x < 1$) including the values obtained in this work is reported in Fig. 3.

Table 3
Fractional atomic coordinates and isotropic displacement parameters of $V_{1.1}Mo_{0.9}O_5$

Atom	Wyckoff	x	y	z	B_{iso} (Å^2)	Occ.
Mo	4*i*	0.1473(2)	0	0.0902(5)	0.50(2)	0.45(1)
V	4*i*	0.1473(2)	0	0.0902(5)	0.50(2)	0.55(1)
O1	2a	0	0	0	0.2(2)	1
O2	4*i*	0.1835(7)	0.5	-0.007(2)	0.6(2)	1
O3	4*i*	0.1488(7)	0	0.501(2)	1.1(2)	1

Table 4
Space group, cell parameters, selected bond distances (Å) and angles (deg) with their standard deviations for V_2O_5 [19], $V_{2-x}Mo_xO_5$ (according to [1,3,4,6] and this work) and R-Nb_2O_5 [31] (M = Mo, V)

	V_2O_5	$V_{1.7}Mo_{0.3}O_5$	$V_{1.4}Mo_{0.6}O_5$	$V_{1.1}Mo_{0.9}O_5$	R-Nb_2O_5
Space group	*Pmmn*	*Pmmn*	*C*2	*C*2/*m*	*C*2/*m*
a (Å)	11.512(3)	11.679(6)	11.809(2)	12.1230(2)	12.79(1)
b (Å)	3.564(1)	3.600(2)	3.652(1)	3.7168(1)	3.826(4)
c (Å)	4.368(1)	4.260(2)	4.174(1)	4.0336(1)	3.983(4)
β (°)			90.56(2)	90.625(1)	90.75(5)
V (Å^3)	179.2(1)	179.1(3)	180.0(1)	181.73(1)	194.9(4)
M–O1	1.779(3)		1.804(3)	1.818(2)	1.89(3)
M–O2	1.878(1)		1.73(4)	1.950(2)	1.98(4)
M–O2^{i}	1.878(1)		2.09(4)	1.950(2)	1.98(4)
M–O2^{ii}	2.017(3)		2.08(2)	2.082(5)	2.2(1)
M–O3	1.577(3)		1.659(2)	1.656(6)	1.7(2)
M–O3^{iii}	2.791(3)		2.54(2)	2.377(6)	2.3(2)
M–*M*^{ii}	3.082(1)		3.126(1)	3.198(2)	3.33(3)
M–O1–*M*^{iv}	3.56(1)		3.607(1)	3.636(2)	3.76(4)
O2–*M*–O2^{ii}	75.5(1)		80.4	75.1(2)	76.3(4)
O2^{i}–*M*–O2^{ii}	75.5(1)		72.7	75.1(2)	76.3(4)
O1–*M*–O2	97.1(1)		98.5	100.5(2)	101.4(4)
O1–*M*–O2^{i}	97.1(1)		96.6	100.5(2)	101.4(4)

Symmetry codes related to the description of the $V_{1.1}Mo_{0.9}O_5$ structure in space group *C*2/*m*: $^{i}x, -y, z$; $^{ii}-x+0.5, y-0.5, -z$; $^{iii}x, y, -z$; $^{iv}-x, y, -z$.

An important fact to notice is the shortening of the *c* parameter which allows the successive apical oxygen planes of the $[M_2O_5]_n$ layers to interpenetrate and then to transform the orthorhombic V_2O_5 and monoclinic $V_{1.4}Mo_{0.6}O_5$ layer structures into a 3D one. In V_2O_5 it has been clearly demonstrated that the space Δ (Fig. 2) between two successive apical oxygen planes is distant by some $+0.27$ Å [9,19]. The introduction of increasing amounts of Mo in V_2O_5 reduces the long interatomic distance M–O3 = 2.791(3) Å (see Table 4) inducing the reversal of the double string of MO_5 square pyramids and the reduction of the *c* parameter. The distance M–O3 becomes 2.54(2) Å and the space between the O3 successive planes decreases to $\Delta = +0.06$ Å in the monoclinic $V_{1.4}Mo_{0.6}O_5$ phase, which can still be considered as a layer structure. In the new phase $V_{1.1}Mo_{0.9}O_5$, we assist in the interpenetration of the layers with $\Delta = -0.01$ Å (M–O3 = 2.377(6) Å). The previous packing of the $[M_2O_5]_n$ layers held by Van der Waals interactions and counterbalanced by the O3 successive planes repulsions allows now the M–O3 bond to be established, strengthening the network. This latter is then more closely related to the one of R-Nb_2O_5.

The evolution of the other cell parameters with Mo content is explained by fine structural details. Their increase is connected to the M–M interatomic distances in the (*a*, *b*) plane: in the same double string, the M–M distance is 3.082(1) Å in V_2O_5 while it becomes equal to 3.126(1) and 3.198(2) Å in $V_{1.4}Mo_{0.6}O_5$ and $V_{1.1}Mo_{0.9}O_5$, respectively. The M–O1–M distances, which correspond to the sum of the two M–O1 bonds linking the double strings between them, directly result in increasing the *a* cell parameter. These distances go from 3.56(1) Å in V_2O_5 to 3.607(1) Å in $V_{1.4}Mo_{0.6}O_5$ to finally reach 3.636(2) Å in $V_{1.1}Mo_{0.9}O_5$. This is directly related to the ionic radii of Mo(VI) and V(IV) which are essentially identical in octahedral coordination (0.59 and 0.58 Å, respectively) compared to 0.54 Å for V(V) in the same coordination [32]. Moreover, we can reasonably assume that the charge of the Mo(VI) is responsible for the expansion of the (*a*, *b*) plane, the repulsion between metallic centers being enlarged with the substitution of Mo(VI) + V(IV) for V(V) in V_2O_5.

It is also interesting to note that the MO_6 octahedra are slightly less distorted in $V_{1.1}Mo_{0.9}O_5$ than in $V_{1.4}Mo_{0.6}O_5$ with the in-plane M–O bond distances varying between 1.818(2) and 2.082(5) Å in $V_{1.1}Mo_{0.9}O_5$ in comparison with

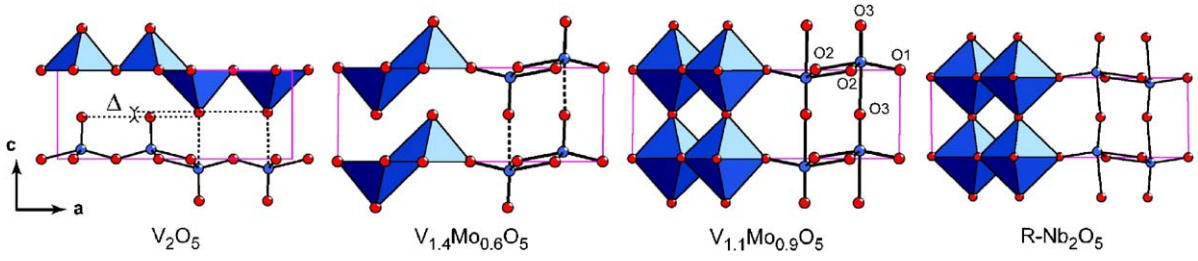

Fig. 2. Comparative view of the (*a*, *c*) plane of the V_2O_5, $V_{1.4}Mo_{0.6}O_5$, $V_{1.1}Mo_{0.9}O_5$ and R-Nb_2O_5 compounds.

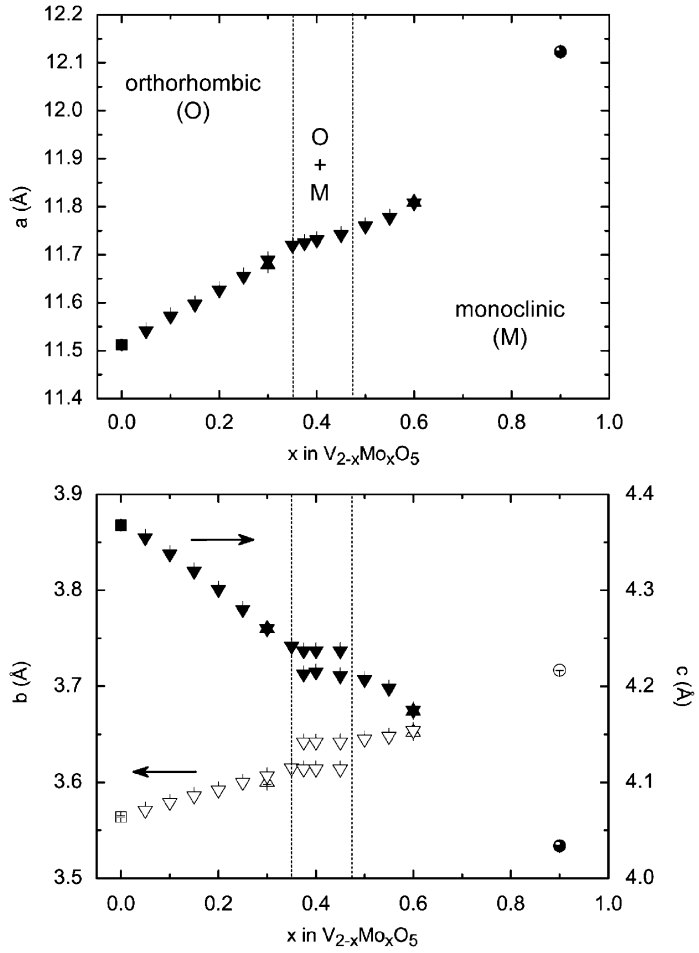

Fig. 3. Cell parameters of the $V_{2-x}Mo_xO_5$ phases as a function of the Mo content. Only the phases obtained by solid-state reactions are reported with the one prepared in this work. In the lower graph, open symbols correspond to the *b* cell parameter whereas filled symbols relate to the *c* parameter. Square symbols refer to [19], triangular ones (up and down) correspond to Refs. [1,3,4,6,8], circle ones to this work.

1.73(4) and 2.09(4) Å in $V_{1.4}Mo_{0.6}O_5$. This fact is linked to the very small remaining amount of V(V) which always induces tremendous distortions in its coordination polyhedron. In $V_{1.4}Mo_{0.6}O_5$, the V(V) is predominant as it can be seen in its cationic formulation $[V(V)_{0.8}V(IV)_{0.6}Mo(VI)_{0.6}O_5]$.

To sum up, this structural analysis shows that $V_{1.1}Mo_{0.9}O_5$ follows the trends previously observed in the cell parameters and the structure of the $V_{2-x}Mo_xO_5$ phases obtained by solid-state reactions ($0.48 \leqslant x \leqslant 0.60$). The structure of this compound, although it is 3D, is more closely related to the monoclinic layer structure of this solid solution than to the tetragonal one of $[V(IV)Mo(VI)O_5]$ [14,18] in spite of their nearest chemical formula. Even if it is difficult to give a direct proof of the presence of V(V) because of its small quantity in the compound, the cell parameters obtained for the various powders prepared by hydrothermal synthesis (Table 1) from an excess of $VOSO_4$ compared to the molybdenum-based reagent ($HoMoO_4$) seem to indicate the existence of such a solid solution. As a matter of fact, the *a* parameter of these compounds seems to be more sensitive to determine any variation of V/Mo ratio (Fig. 3). When this ratio ranges from 1.06 to 1, the variation of the *a* parameter reaches about 0.02 Å compared to 0.03–0.04 Å for a V/Mo ratio equal to 1.5 or 2 (Table 1). This fact is definitely in favour of a composition with a mixed valence (V(IV), V(V)) since a slight increase of the vanadium content in the final product necessarily leads to a greater quantity of V(V). Further synthesis and characterizations would be needed in order to determine accurately the homogeneity range of this solid solution at these soft chemistry conditions. The remarkable versatility and ability of Mo(VI), V(V) and V(IV) to adopt in their various oxidation states the same types of coordination polyhedra, namely CN5 (square pyramids or trigonal bipyramids) and CN6 (distorted octahedra), are probably responsible for the stabilization of this phase in this symmetry.

Finally, we can conclude that the preparation by soft hydrothermal techniques provides more relaxed conditions allowing the introduction of a bigger amount of Mo and leading to the formation of this new phase. This result clearly indicates that it should be possible, by means of hydrothermal synthesis, to extend the homogeneity range of the monoclinic solid solution which is restrained to $0.48 \leqslant x \leqslant 0.60$ at 600–650 °C. This could probably also be

possible to achieve by solid-state reactions performed at lower temperatures (i.e. between 450 and 550 °C).

Supplementary material

Further details of the crystal structure investigation can be obtained from the Fachinformationszentrum Karlsruhe, 76344 Eggenstein-Leopoldshafen, Germany (fax: +49 7247 808 666; e-mail: crysdata@fiz.karlsruhe.de) on quoting the depository no. CSD-416494.

Acknowledgments

The authors would like to thank Jean Galy for valuable suggestions and discussions.

References

[1] H.A. Eick, L. Kihlborg, Nature 211 (1966) 515–516.
[2] J. Galy, J. Darriet, D. Canals, C. R. Acad. Sci. 264 (1967) 1477–1481.
[3] J. Darriet, Etude cristallochimique de nouveaux dérivés de substitution des bronzes oxygénés de vanadium, Thesis, Université de Bordeaux, Bordeaux, 1971.
[4] J. Darriet, J. Galy, P. Hagenmuller, J. Solid State Chem. 3 (1971) 596–603.
[5] J. Darriet, J. Galy, P. Hagenmuller, J. Solid State Chem. 3 (1971) 604–613.
[6] L. Kihlborg, Acta Chem. Scand. 21 (1967) 2495–2502.
[7] J. Galy, F. Duc, G. Svensson, P. Baules, P. Rozier, P. Millet, Solid State Sci. 7 (2005) 726–734.
[8] P. Rozier, private communication.
[9] J. Galy, J. Solid State Chem. 100 (1992) 229–245.
[10] T. Chirayil, P.Y. Zavalij, M.S. Whittingham, Chem. Mater. 10 (1998) 2629–2640.
[11] P.J. Hargrman, R.C. Finn, J. Zubieta, Solid State Sci. 3 (2001) 745–774.
[12] F. Haaß, A.H. Adams, T. Buhrmester, G. Schimanke, M. Martin, H. Fuess, Phys. Chem. Chem. Phys. 5 (2003) 4317–4324.
[13] A.H. Adams, F. Haaß, T. Buhrmester, J. Kunert, J. Ott, H. Vogel, H. Fuess, J. Mol. Catal. A: Chem. 216 (2004) 67–74.
[14] H.A. Eick, L. Kihlborg, Acta Chem. Scand. 20 (1966) 722–729.
[15] P. Carretta, N. Papinutto, C.B. Azzoni, M.C. Mozzati, E. Pavarini, S. Gonthier, P. Millet, Phys. Rev. B 66 (2002) Art. No. 094420.
[16] P. Carretta, N. Papinutto, C.B. Azzoni, M.C. Mozzati, E. Pavarini, S. Gonthier, P. Millet, Acta Phys. Pol. B 34 (2003) 1407–1410.
[17] A. Bombardi, L.C. Chapon, I. Margiolaki, C. Mazzoli, S. Gonthier, F. Duc, P.G. Radaelli, Phys. Rev. B 71 (2005) Art. No. 220406.
[18] S. Gonthier, Systèmes modèles du réseau carré frustré—Synthèse, caractérisations structurales et propriétés magnétiques—Etude en fonction de la température, Thesis, Université Paul Sabatier, Toulouse, 2005.
[19] R. Enjalbert, J. Galy, Acta Crystallogr. C 42 (1986) 1467–1469.
[20] A.N. Fitch, J. Res. Natl. Inst. Stand. Technol. 109 (2004) 133–142.
[21] T. Roisnel, J. Rodriguez-Carvajal, Mater. Sci. Forum 378–381 (2000) 118–123.
[22] A. Boultif, D. Louër, J. Appl. Crystallogr. 37 (2004) 724–731.
[23] A. Altomare, C. Giacovazzo, A. Guagliardi, A.G.G. Moliterni, R. Rizzi, P.E. Werner, J. Appl. Crystallogr. 33 (2000) 1180–1186.
[24] J. Rodriguez-Carvajal, FULLPROF: a program for Rietveld refinement and pattern matching analysis, in: Collected Abstracts of Powder Diffraction Meeting, Toulouse, France, 1990, pp. 127–128.
[25] K. Brandenburg, DIAMOND (Version 3.1a), Crystal Impact GbR, Bonn, Germany, 1997–2005.
[26] L.M. Plyasova, L.P. Solov'eva, S.V. Tsybulya, G.N. Kryukova, V.A. Zabolotnyi, I.P. Olen'kova, Zh. Strukt. Khim. 32 (1991) 110–115.
[27] P.M. de Wolff, J. Appl. Crystallogr. 1 (1968) 108–113.
[28] A. Altomare, G.L. Cascarano, C. Giacovazzo, A. Guagliardi, A.G.G. Moliterni, M.C. Burla, G. Polidori, J. Appl. Crystallogr. 28 (1995) 738–744.
[29] L.W. Finger, D.E. Cox, A.P. Jephcoat, J. Appl. Crystallogr. 27 (1994) 892–900.
[30] M. Occhiuzzi, D. Cordischi, R. Dragone, J. Solid State Chem. 178 (2005) 1551–1558.
[31] R. Gruehn, J. Less-Common Met. 11 (1966) 119–126.
[32] R.D. Shannon, Acta Crystallogr. A 32 (1976) 751–767.